RSC Advances

REVIEW

View Article Online
View Journal | View Issue

Cite this: *RSC Adv.*, 2022, **12**, 251

Synthetic strategy and structure–activity relationship (SAR) studies of 3-(5′-hydroxymethyl-2′-furyl)-1-benzyl indazole (YC-1, Lificiguat): a review

Ko-Hua Yu and Hsin-Yi Hung *

Received 5th November 2021
Accepted 14th December 2021

DOI: 10.1039/d1ra08120a

rsc.li/rsc-advances

Since 1994, YC-1 (Lificiguat, 3-(5′-hydroxymethyl-2′-furyl)-1-benzylindazole) has been synthesized, and many targets for special bioactivities have been explored, such as stimulation of platelet-soluble guanylate cyclase, indirect elevation of platelet cGMP levels, and inhibition of hypoxia-inducible factor-1 (HIF-1) and NF-κB. Recently, Riociguat®, the first soluble guanylate cyclase (sGC) stimulator drug used to treat pulmonary hypertension and pulmonary arterial hypertension, was derived from the YC-1 structure. In this review, we aim to highlight the synthesis and structure–activity relationships in the development of YC-1 analogs and their possible indications.

1. Introduction

YC-1 (Lificiguat, 3-(5′-hydroxymethyl-2′-furyl)-1-benzyl indazole) is an indazole derivative whose structure contains furyl and benzyl substituents at positions 1 and 3 (Fig. 1). In 1994, YC-1 was first synthesized and reported by Kuo's group and exhibited antiplatelet activity with a 70% inhibition of platelet aggregation induced at a concentration of 30 μmol L^{-1}.[1,2] YC-1 is a potential antiplatelet agent for prevention and treatment of vascular embolisms. The mechanisms of action of the antiplatelet activity of YC-1 include direct stimulation of platelet-soluble guanylate cyclase (sGC) and indirect elevation of platelet cyclic guanosine monophosphate (cGMP) levels.[1] Since the discovery of YC-1 in 1994, many other molecular targets of YC-1 have been identified. YC-1 is a hypoxia-inducible factor-1 (HIF-1) inhibitor[3,4] that exhibits anticancer activities,[5–7] reverse chemoresistance,[8,9] retinal neovascularization inhibition,[10,11] neural protection[12,13] and decreased allergic inflammatory gene expression.[14] In addition, Carroll *et al.*[15] found that YC-1 displays inhibitory activity against vascular endothelial growth factor (VEGF) for treating inflammation.[16] Additionally, YC-1 was found to inhibit the activity of the nuclear factor kappa light chain enhancer of activated B cells (NF-κB),[17] which is a critical signaling pathway for learning and memory,[18] as well as bone formation.[19]

The structure–activity relationship (SAR) of YC-1 and its derivatives have been studied in the past decade. However, in the past reviews[20,21] of YC-1, only the relevant pharmacological activities were discussed, leaving open the synthesis strategy and SAR. Some valuable YC-1 derivatives have even been developed into clinical drugs, such as Riociguat. Riociguat, whose structure is based on YC-1, is a clinical drug indicated for pulmonary artery hypertension (PAH) *via* stimulating soluble guanylate cyclase (sGC). Thus, we mainly focus on the chemical synthesis of YC-1, the synthesis of its derivatives, and discussion of the SAR in this review.

Based on an overview of all the chemical syntheses for YC-1 and its derivatives, the starting materials are easily available and, inexpensive raw materials.[2,22–24] The derivatives are modified mainly on the functional groups in aromatic and furyl rings and the number of nitrogen atoms. The chemical modification reactions comprise reduction, oxidation, esterification, substitution reactions, Suzuki coupling, and direct arylation. In the following section of this review, we comprehensively describe the synthetic methods, biological activities, and the SAR of YC-1 and summarize the most effective structure for various biological activities (HIF-1, sGC, VEGF and NF-κB), which will be beneficial for future research and development of YC-1 derivatives with optimized bioactivity.

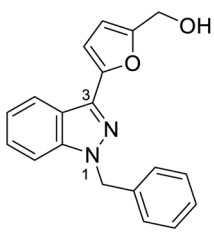

YC-1, 1

Fig. 1 Structure of YC-1 (1).

School of Pharmacy College of Medicine, National Cheng Kung University, Tainan 701, Taiwan. E-mail: z10308005@email.ncku.edu.tw

2. Synthetic strategies of 3-(5′-hydroxymethyl-2′-furyl)-1-benzyl indazole (YC-1) and YC-1 derivatives

The synthesis of YC-1 derivatives has attracted considerable attention in organic and medicinal chemistry due to their excellent bioactivities. Different synthetic strategies have been developed depending on the desired chemical structure. Here, we summarize several synthetic strategies used in the synthesis of YC-1 (Scheme 1).

The synthesis of YC-1 was first described by Teng *et al.* (2002).[25,26] Their synthetic plan started from benzoyl chloride and ethyl furan-2-carboxylate catalyzed by ferric chloride to obtain carbonyl coupling compound **4** (route a). Then, methyl 5-benzoylfuran-2-carboxylate (**4**) was converted to hydrazine compound **5** using benzyl hydrazine and acetic acid. Compound **5** underwent a cyclization reaction catalyzed by lead(IV) acetate [$Pb(OAc)_4$] and then boron trifluoride (BF_3) to obtain compound **6**. Finally, the ester group was reduced to a hydroxyl group *via* calcium borohydride [$Ca(BH_4)_2$] to yield the final compound **1** (YC-1), and the total yield was 4.3%.

In the original synthesis route of YC-1, the corresponding indazole from cyclization of the hydrazine compound had several drawbacks, including too many steps, use of organic metal reagents, and low yield. Collot *et al.*,[27] Hering *et al.*[28] and Takeuchi *et al.*[22] modified the synthetic process of YC-1 starting from indazole (**9**) (route b).[29] First, indazole mixed with iodine (I_2), and potassium hydroxide (KOH) in dimethylformamide (DMF) was used to install the iodo group at position 3. Next, benzyl bromide (BnBr), potassium *tert*-butoxide (*t*-BuOK), and tetrabutylammonium iodide (Bu_4NI) in tetrahydrofuran (THF) were reacted with compound **10** to obtain benzyl substituent **11**. Hering[28] and Takeuchi[22] prepared YC-1 *via* stannane reaction using palladium catalysis from 1-benzyl-3-iodoindazole, and the yield increased to 74%. However, organostannanes are generally considered inappropriate for drug synthesis due to their toxicity. Collot avoided organostannane reagents. Instead, Suzuki coupling reaction of **11** with boronic acid substituted with aromatic compound (**12**) was carried out to obtain **13** by Vilsmeier–Haack reaction.[27] Reduction of the formyl group with sodium borohydride was applied to obtain YC-1, and the yield improved to 79%.

Even though the yield improved to above 70%, there were still doubts about the use of heavy metals in the total synthesis. Hence, in 2008, Carla *et al.* developed a synthesis method that did not involve the use of heavy metals.[24,30] In this report, all of the reagents used were less toxic and less expensive than those used in previous studies (route d). The starting materials were 2-aminobenzoic acid (**20**) and furan, which reacted with *n*-butyllithium in THF to obtain carbonyl compound **21.** Compound **21** reacted with hydroxylamine hydrochloride to give oxime compound **22**, which underwent a cyclization reaction using methanesulfonyl chloride (MsCl) to give compound **19**. The

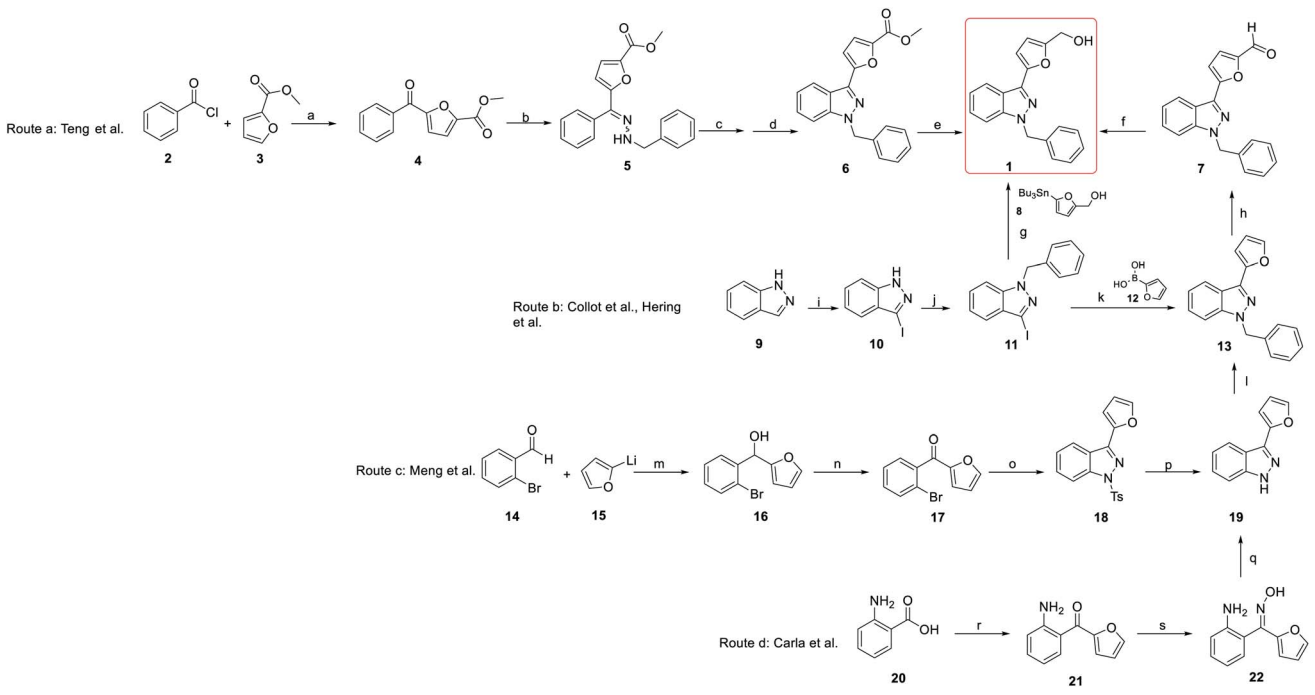

Scheme 1 Summary of synthesis of YC-1 (**1**). Route a: synthesis by Teng *et al.* (2002); route b: synthesis by Collot *et al.* and Hering *et al.* (1999, 2006); route c: synthesis by Meng *et al.* (2017); route d: synthesis by Carla *et al.* (2008). Reagents and conditions: (a) $FeCl_3$; (b) $PhCH_2NHNH_2$, HOAc; (c) $Pb(OAc)_4$; (d) BF_3Et_2O; (e) $Ca(BH_4)_2$; (f) $NaBH_4$, MeOH, rt; (g) $Pd_2(dba)_3$, $AsPh_3$, DMF; (h) $POCl_3$, DMF, 0 °C to 80 °C; (i) I_2, KOH, DMF; (j) BnBr, *t*-BuOK, Bu_4NI, THF; (k) $Pd(PPh_3)_4$, $NaHCO_3$, DME, reflux; (l) $ArCH_2Br$, *t*-BuOK, THF, 0 °C to rt; (m) THF, −80 °C; (n) MnO_2, CH_2Cl_2; (o) (i) $TsNHNH_2$, HCl, MeOH; (ii) Cu_2O, i-AmOH, reflux; (p) Mg, MeOH; (q) MsCl, Et_3N, CH_2Cl_2; (r) furan, *n*-BuLi, THF, −78 °C to 0 °C; (s) HO–NH_2 HCl, pyridine, MeOH, reflux.

final product, YC-1, was prepared following formylation and reduction of compound **19**.[27] This synthetic route not only reduced heavy metal usage but also retained the total yield.

In addition, in 2004 and 2007, Inamoto *et al.*[31] and Sakamoto *et al.*[32] reported the first method for preparing indazole through intramolecular cyclization of Pd-catalyzed *ortho*-bromine tosylhydrazone under the action of a base and ligand. However, the reaction must be carried out under alkaline conditions, and compound **24** was formed by Bamford–Stevens reaction, where the *E*-form was the main product. The *E*-form isomer cannot obtain the corresponding product (**25**); in contrast, the *Z*-form can give better reaction results (Scheme 2). In 2017, Meng *et al.* pointed out for the first time that indazole (**25**) can be obtained by the reaction of an *E*-form or *Z*-form tosylhydrazone isomer with cuprous oxide (Cu_2O) by heating (Scheme 2), which is suitable for a variety of functional groups and has an extremely high yield.[23]

Meng's group also reported another synthetic strategy (Scheme 1, route c) based on 2-bromobenzaldehyde (**14**). (2-Bromophenyl)(furan-2-yl)methanone (**17**) was prepared through affinity addition and oxidation, after which it was cyclized by tosylhydrazone to form indazole compound **18**. Removing tosyl and adding benzyl groups was obtained compound **19**. Subsequently, **19** was subjected to Vilsmeier–Haack reaction and reduced to obtain YC-1 (**1**).

3. Structure–activity relationship (SAR) result of YC-1

3.1. Soluble guanylate cyclase (sGC)

YC-1 was first discovered as a novel sGC stimulator that is influenced by NO or NO donors.[33] Upon sGC stimulation, several physiological events occur, including inhibition of the contraction of vascular smooth muscles and inhibition of platelet adhesion and aggregation.[2,34] YC-1 may also potentiate the action of endogenous and exogenous carbon monoxide (CO) on sGC and stimulate sGC with NO in a synergistic manner. In addition, administration of YC-1 may affect age-related learning and memory dysfunction *via* the NO/cGMP signaling pathway, which sGC crucially contributes to.[18,35,36] For example, in Morris water maze (MWM) avoidance response tests, YC-1-treated group (1 mg kg^{-1}) improved rodent learning behavior and performed a higher avoidance response rate in which the mean avoidance response was 18.7% and 33.3% for the control and YC-1-treated rats, respectively, on day 11.[37]

Moreover, YC-1 has been found to have an important regulatory effect on sGC and cGMP signaling in the cardiovascular system, where YC-1 directly stimulates sGC and then activates NO production that subsequently relaxes vascular smooth muscles.[38,39] Furthermore, YC-1 inhibits focal adhesion kinase and proliferative factor transforming growth factor β1 (TCF-β1) to reduce the growth of vascular smooth muscle.[40] In addition, YC-1 prevents oxidized LDL-mediated apoptosis and induces Hsp70 expression.[39]

Due to many stimulate activities related to sGC, the SAR discussion in the next section is divided into two parts: relaxation of vascular smooth muscles and antiplatelet activities.

3.1.1. YC-1 derivatives as sGC stimulator. In all the SAR studies of YC-1, sGC has been the most investigated. Compound inhibition abilities (IC_{50}) were measured by the inhibition of the maximum constriction of phenylephrine-induced pre-constricted rabbit aortic rings[26,41] and the inhibition of sodium nitroprusside (SNP)-induced apoptosis of rat aortic smooth muscle cells.[42] The following SAR research is discussed according to R^1, R^2, heterocycle A and heterocycle B functional groups (Fig. 2).

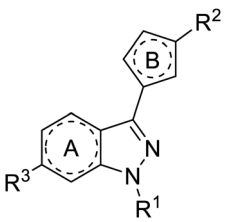

Fig. 2 Generic structure to represent SAR for YC-1.

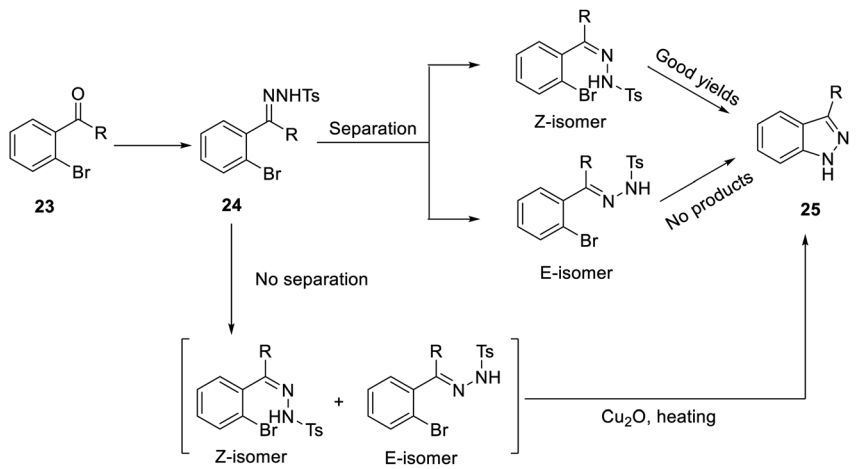

Scheme 2 Synthesis of indazole (**25**), an intermediate of YC-1 synthesis.

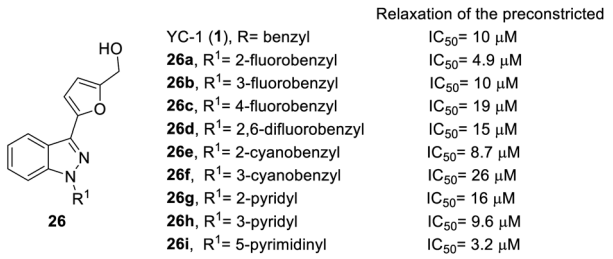

Fig. 3 Effect of 1-*N*-substituted derivatives (**26**) on relaxation of preconstricted aortic rings.

According to the structure of YC-1, Straub *et al.* discussed the SAR based on 1-*N*-substituent whose synthesis followed route b in Scheme 1 and replaced the benzyl bromide functional group to obtain compound **26** (Fig. 3)[26,41]. Among all the derivatives, only fluoro or cyano substitution at the *ortho* position of the benzene ring led to better inhibitory activity, evidenced from **26a** and **26e** (IC_{50} = 4.9 and 8.7 μM, respectively). If the substitution was at the *meta* or *para* position, this inhibitory activity was reduced, such as in compounds **26b**, **26c** and **26f** (IC_{50} = 10, 19 and 26 μM, respectively). The dual substitution of fluoro also reduced inhibition activity, for which the IC_{50} value of **26d** was 15 μM. However, only 5-pyrimidinyl (**26i**) had good inhibitory activity among all of the heterocyclic substitutions (**26g–26i**), where the IC_{50} value was 3.2 μM. According to the results shown in Fig. 3, the substituted position of fluoro or cyano plays an important role in the relaxation of preconstricted aortic rings.

In the core structure of YC-1 (heterocycle A), Straub *et al.* studied the impact of different cores on relaxation effects on preconstricted aortic rings (Fig. 4).[26,41] The synthesis of compound **27** followed route b in Scheme 1 and replaced the indazole starting material. The results showed that more nitrogen atoms in the heterocycles contributed to little increases in inhibitory activity (**27f**, IC_{50} = 9.4 μM). The most effective compound was pyrazolopyridinyl pyrimidine (**27b**), with an IC_{50} value of 1.7 μM. Unfortunately, other pyrazolopyridine derivatives exhibited inferior activities, such as **27c**, **27d** and **27e** (IC_{50} values of 6.9, 9.8, and 20.4 μM, respectively). Therefore, the position of nitrogen has a close relationship with inhibitory activity. A compound with 1*H*-pyrazolo[4,3-*c*]pyridine (**27b**) was found to be more potent than one with indazole (**27a**) in the core structure.

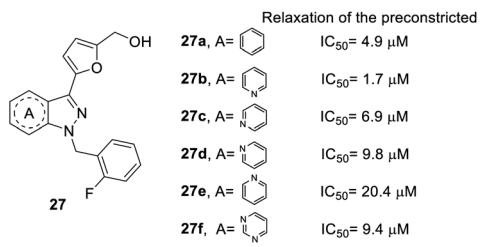

Fig. 4 Effect of YC-1 derivatives (**27**) on relaxation of preconstricted aortic rings.

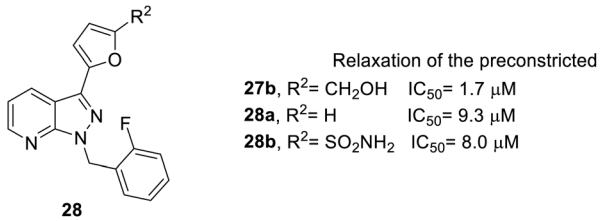

Fig. 5 Effect of YC-1 derivatives (**28**) on relaxation of preconstricted aortic rings.

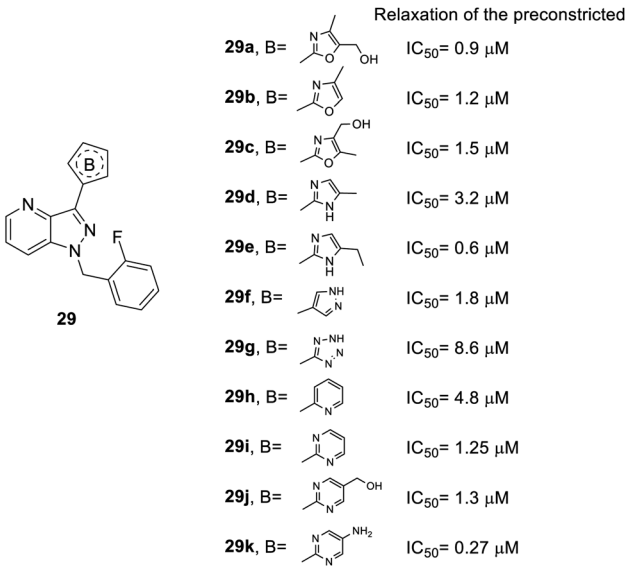

Fig. 6 Effect of heterocycle B-substituted YC-1 derivatives (**29**) on relaxation of preconstricted aortic rings.

Next, when R^2 was substituted as compound **28**, whose synthesis followed Scheme 1, route b, only the hydroxymethyl side chain retained inhibitory activity (Fig. 5). For example, compound **27b** with a hydroxymethyl side chain resulted in good inhibitory activity (IC_{50} = 1.7 μM), but the inhibitory activity was reduced (IC_{50} = 9.3 and 8.0 μM, respectively) when the hydroxymethyl group was replaced with hydrogen (**28a**) or sulfonamide (**28b**).

As for heterocycle B, the synthesis of the derivatives followed route b in Scheme 1 and replaced compound **12** to other

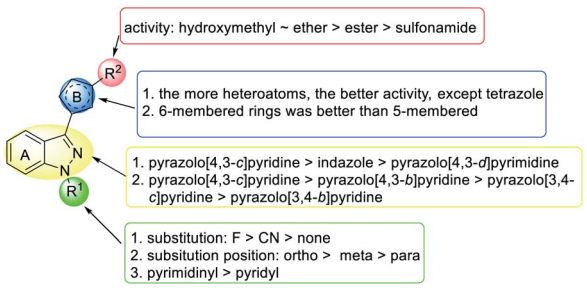

Fig. 7 SAR of YC-1 analogs on relaxation of preconstricted aortic rings.

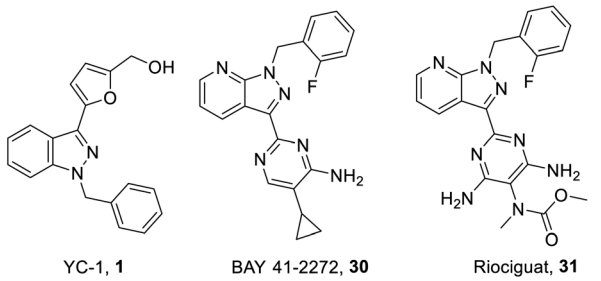

Fig. 8 Structure of YC-1 (**1**), BAY 41-2272 (**30**) and Riociguat (**31**).

heterocycles. When the furan ring of compound **28** was replaced with isoxazole (**29a–c**), 1*H*-pyrazole (**29d–e**) or other heterocycles (**29f–k**), better inhibitory effects were observed (Fig. 6). For instance, the isoxazole of compound **29a–c** (IC_{50} = 0.9, 1.2 and 1.5 μM, respectively) and 1*H*-pyrazole of compound **29e** (IC_{50} = 0.6 μM) manifested better activity than the furan-substituted functional group (**28b**, IC_{50} = 1.7 μM). Furthermore, dinitrogen-containing heterocycles B [imidazole (**29e–f**) and pyrimidine (**29i–k**)] increased inhibitory performance (IC_{50} = 0.6, 1.8, 1.25, 1.3 and 0.27 μM, respectively). However, tetrazole-substituted **29g** significantly reduced this activity (IC_{50} = 8.6 μM).

In summary (Fig. 7), in terms of the core structure, the best structure is pyrazolopyridinyl pyrimidine, which further develops into Riociguat. At R^1, the best substituent is the *ortho* fluoro benzyl group. The best substituent for the R^2 position is a hydroxymethyl or ether group, and the worst is sulfonamide. The presence of pyrimidine ring as A ring as well as R^1 substitution gave considerable IC_{50} values in compounds, **27b**, **26i**, **29e**, and **29k**. More nitrogen-substituted rings have shown enhancement in activity for relaxation effects on preconstricted aortic rings. In the ring B position, heterocycles are generally effective except for tetrazole, and 6-membered rings are better than 5-membered rings (Fig. 7).

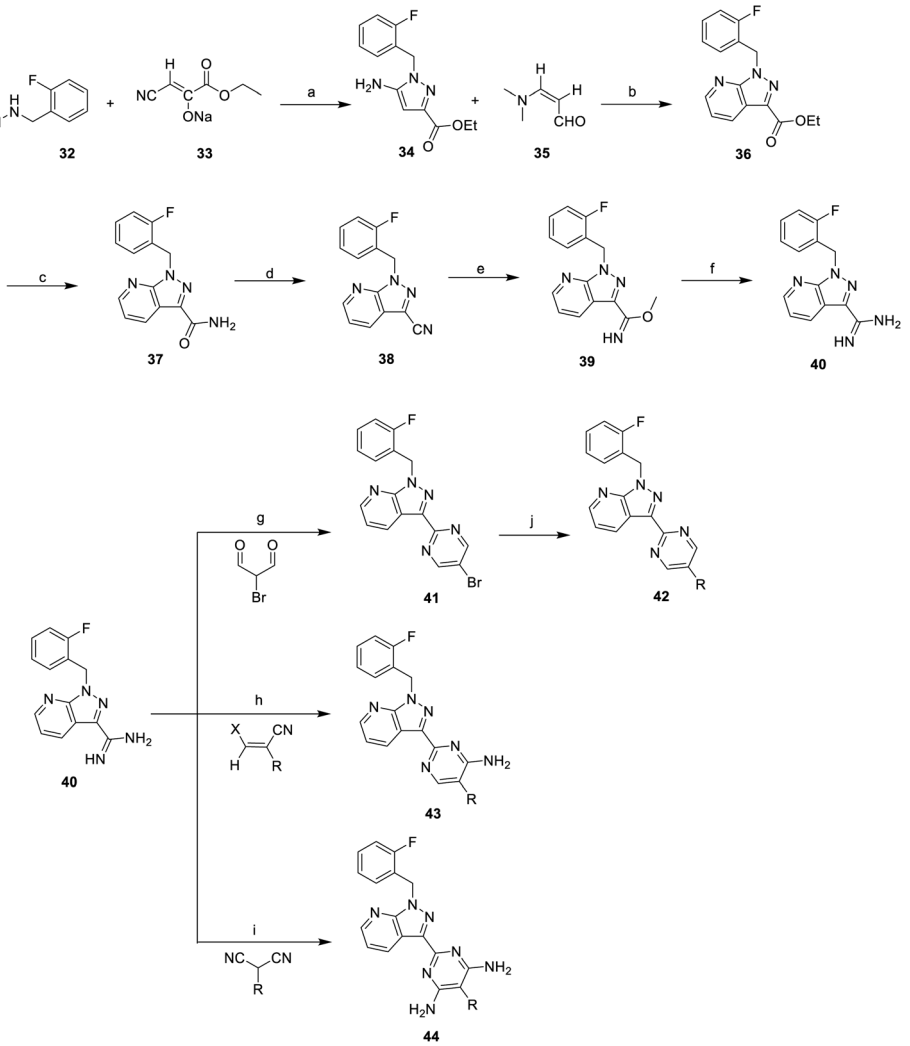

Scheme 3 Synthesis of YC-1 analogs (**42–44**). Reagents and conditions: (a) TFA, 1,4-dioxane, reflux, 8 h; (b) TFA, 1,4-dioxane, reflux, 3 days; (c) NH_3/MeOH, rt, 2 days; (d) TFAA/pyridine, pyridine, rt, 8 h; (e) MeONa/MeOH, rt, 2 h; (f) and (i) NH_4Cl/HOAc, MeOH, reflux, 8 h; (ii) Na_2CO_3/H_2O, rt; (g) HOAc, 100 °C, 2 h; (h) toluene, reflux, overnight; (j) *t*-BuOK, [Pd_2dba_3], (*rac*)-BINAP, toluene, 70 °C, overnight; (i) neat, 105 °C, slight vacuum, 3–12 h.

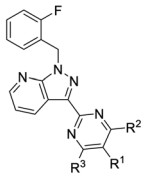

				Relaxation of the preconstricted
42,	R^1= *N*-morpholino;	R^2=H;	R^3=H	IC_{50}= 0.93 μM
43a,	R^1= Et;	R^2=NH_2;	R^3=H	IC_{50}= 0.27 μM
43b,	R^1= *N*-morpholino;	R^2=NH_2;	R^3=H	IC_{50}= 0.26 μM
43c,	R^1= *n*-propyl;	R^2=NH_2;	R^3=H	IC_{50}= 0.25 μM
43d,	R^1= *n*-hexyl;	R^2=NH_2;	R^3=H	IC_{50}= 1.04 μM
43e,	R^1= *t*-butyl;	R^2=NH_2;	R^3=H	IC_{50}= 0.71 μM
43f,	R^1= cyclopropyl;	R^2=NH_2;	R^3=H	IC_{50}= 0.30 μM
43g,	R^1= cyclopentyl;	R^2=NH_2;	R^3=H	IC_{50}= 0.90 μM
43h,	R^1= CN;	R^2=NH_2;	R^3=H	IC_{50}= 0.39 μM
43i,	R^1= 6-cyanoheptyl;	R^2=NH_2;	R^3=H	IC_{50}= 1.29 μM
43j,	R^1= OCH_3;	R^2=NH_2;	R^3=H	IC_{50}= 0.34 μM
43k,	R^1= F;	R^2=NH_2;	R^3=H	IC_{50}= 0.48 μM
44a,	R^1= Et;	R^2= NH_2;	R^3=NH_2	IC_{50}= 0.11 μM
44b,	R^1= *N*-morpholino;	R^2= NH_2;	R^3=NH_2	IC_{50}= 0.10 μM
44c,	R^1= cyclopropyl;	R^2= NH_2;	R^3=NH_2	IC_{50}= 0.23 μM

Fig. 9 Effects of pyrazolopyridinyl pyrimidine derivatives on relaxation of preconstricted aortic rings.

On the other hand, one of the YC-1 derivatives (Bay 41-2272, **30**,) Fig. 8 has been developed into a clinically used drug by Bayer Pharmaceuticals as a new pyrazolopyridinyl pyrimidine derivative (Riociguat, **31**). This drug acts on the NO-sGC-cGMP pathway to effectively dilate blood vessels and inhibit smooth muscle hyperplasia. The synthesis of Riociguat-like, pyrazolopyridinyl pyrimidine derivatives was published in a report in 2009 by Mittendorf *et al.* (Scheme 3).[43]

Mittendorf *et al.* started from ethyl cyanopyruvate (**33**) and 2-fluorobenzylhydrazine (**32**) to generate aminopyrazole (**34**). The subsequent 3-dimethylaminoacrolein (**35**) underwent cyclocondensation to give pyrazolopyridine **36** with a 50% overall yield. Then, the ester group of **39** was transformed into an amide using ammonia in methanol and reacted with trifluoroacetic anhydride (TFAA) to give cyano compound **38**. Compound **38** underwent a pinner reaction with sodium methoxide, followed by substitution with ammonium chloride to give **40**. Condensation of amidine compound **40** and 2-bromomalondialdehyde in acetic acid resulted in 4,6-unsubstituted **41**; then, Buchwald–Hartwig reaction was applied to obtain morpholine substituted compound **42**. In addition, amidine compound **40** reacted with alkyl-substituted malonic dinitrile under neat conditions to obtain diaminopyrimidines (**43**) with a yield of 40–70%. The nitrile compounds were transformed into the corresponding enol ether. Condensation of the enol ether and amidine **40** yielded **44**. The structure–activity relationship of the pyrazolopyridinyl pyrimidine derivatives (**42–44**) are discussed later in this work.

The development of Bay 41-2272 and Riociguat were based on the SAR results mentioned above, and sGC stimulator **29k** with pyrazolopyridinyl pyrimidine structure was identified and found to be suitable for further research. The results for additional pyrazolopyridinyl pyrimidine derivatives on the relaxation of preconstricted aortic rings are shown in Fig. 9.[43] Overall, pyrazolopyridinyl pyrimidine derivatives (**42–44**) are more active than YC-1. In most cases, the diamino analogs (**44**) are slightly more potent than their monoamino (**43**) counterparts. For example, the inhibitory effect of **44a** (IC_{50} = 0.11 μM), a diamino analog, is better than that of monoamino compound **43a** (IC_{50} = 0.27 μM). The same pattern was observed for compounds **43b**/**44b** and **43f**/**44c**. At the R^1 position of **42–44**, a smaller steric group led to better inhibitory activity. *n*-Propyl substituted **43c**

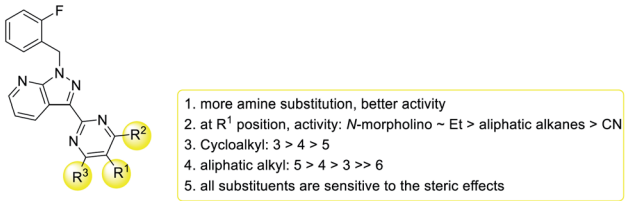

Fig. 10 SAR of pyrazolopyridinyl pyrimidine derivatives on relaxation of preconstricted aortic rings.

(IC_{50} = 0.25 μM) exhibited better inhibitory activity than *n*-hexyl substituted **43d** (IC_{50} = 1.04 μM). The bulky *t*-butyl substituted **43e** reduced inhibitory activity (IC_{50} = 0.71 μM). In addition, cyclic substitution, such as cyclopropyl **43f** (IC_{50} = 0.30 μM) and cyclopentyl **43g** (IC_{50} = 0.90 μM) also decreased potency. However, conversion of an alkyl group to cyano substitution (**43h**) slightly reduced the potency (IC_{50} = 0.39 μM). When installing a linker into **43h** as compound **43i** with a 6-cyanoheptyl substituent, the inhibitory activity was greatly reduced (IC_{50} = 1.29 μM). Furthermore, the electron-donating groups exhibited better activity than the electron-withdrawing substitution. For instance, methoxy substituted **43j** (IC_{50} = 0.34 μM) was superior to the fluoro substituted **43k** (IC_{50} = 0.48 μM).

In summary, the SAR of pyrazolopyridinyl pyrimidine derivatives is shown in Fig. 10. Generally, more amino substituents result in better inhibitory activity. Furthermore, all substituents are sensitive to steric effects. Thus, a smaller cycloalkane or a shorter alkyl led to better activity. At the R^1 position, the best substituents are *N*-morpholino and ethyl, and the worst is cyano substitution.

In addition to the inhibitory activity on preconstricted aortic rings, Lien *et al.* also studied the effects of the derivatives on SNP-induced apoptosis of rat aortic smooth muscle cells (Fig. 11).[42] YC-1 almost completely reversed SNP-induced apoptosis of VSMCs (cell survival: 94.7%) at 30 μM.[42] Conversion of the hydroxymethyl (YC-1, **1**) into ether (**45a**) at the R^2 position retained the activity. Conversion of the hydroxymethyl to amino (**45b**) and diethylamino (**45c**) substitution significantly reduced the activity, while conversion into a methyl group (**45d**) produced a cytotoxic effect in the VSMCs, resulting in a significant reduction in the anti-apoptotic effects. Finally, replacement of the hydroxymethyl by an ester (**45e**) only slightly reduced the activity.[26,41,42]

Insertion of any atom into the YC-1 indazole structure will reduce the cell survival rate.[41] For example, conversion of the R^3

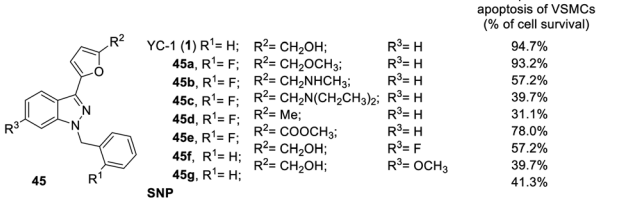

				sodium nitroprusside-mediated apoptosis of VSMCs (% of cell survival)
YC-1 (**1**) R^1= H;	R^2= CH_2OH;	R^3= H		94.7%
45a, R^1= F;	R^2= CH_2OCH_3;	R^3= H		93.2%
45b, R^1= F;	R^2= CH_2NHCH_3;	R^3= H		57.2%
45c, R^1= F;	R^2= $CH_2N(CH_2CH_3)_2$;	R^3= H		39.7%
45d, R^1= F;	R^2= Me;	R^3= H		31.1%
45e, R^1= F;	R^2= $COOCH_3$;	R^3= H		78.0%
45f, R^1= H;	R^2= CH_2OH;	R^3= F		57.2%
45g, R^1= H;	R^2= CH_2OH;	R^3= OCH_3		39.7%
SNP				41.3%

Fig. 11 Anti-apoptotic effect of YC-1 derivatives (**45**) on the sodium nitroprusside-mediated apoptosis of VSMCs.

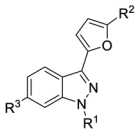

46

				Thrombin	AA	Collagen	PAF	
YC-1 (**1**), R^1= Bn;	R^2= CH_2OH;	R^3= H	IC_{50}	173.0	54.33	53.8	87.3	μM
46a, R^1= Ph;	R^2= CH_2OH;	R^3= H	IC_{50}	158.2	17.9	13.7	145.4	μM
46b, R^1= Bn;	R^2= CH_2OCH_3;	R^3= H	IC_{50}	143.4	8.2	6.6	25.5	μM
46c, R^1= Bn;	R^2= CH_3;	R^3= H	IC_{50}	39.4	47.3	27.5	39.6	μM
46d, R^1= Bn;	R^2= CH_2NEt_2;	R^3= H	IC_{50}	101.9	55.7	50.4	55.9	μM
46e, R^1= Bn;	R^2= CH_2OH;	R^3= Me	IC_{50}	146.9	49.4	45.9	72.0	μM
45f, R^1= Bn;	R^2= CH_2OH;	R^3= F	IC_{50}	217.4	21.7	25.2	53.4	μM
45g, R^1= Bn;	R^2= CH_2OH;	R^3= OCH_3	IC_{50}	168.3	49.7	46.7	89.2	μM

Fig. 12 Effects of YC-1 derivatives (**46a–e**, **45f–g**) on platelet aggregation induced by thrombin, arachidonic acid (AA), collagen, and platelet-activating factor (PAF).

positions with a bridging dioxomethylene group led to even lower activity (cell survival: 39.7%). Introduction of fluoro (**45f**) or methoxy (**45g**) groups into the R^3 position slightly reduced the potency of the inhibitory VEGF.

3.1.2. YC-1 derivatives as antiplatelet agents. In 2001, Lee *et al.* reported the SAR of YC-1 analogs on antiplatelet activities, as summarized in Fig. 12 and 13.[2]

Conversion of the 1-benzyl group of YC-1 to hydrogen significantly reduced the antiplatelet activity. Thus, aromatic rings are needed at the R^1 position in a broad spectrum of antiplatelet activities.

Conversion of the alcohol group into an ether (**46b**) at the R^2 position resulted in considerably increased activity. In addition, amine-substituted **46d** enhanced the inhibitory activity toward thrombin- and PAF-induced aggregation but was inactive against collagen- and AA-induced aggregation. Introduction of an ester resulted in weak inhibitory antiplatelet activities as high as 300 μM. Finally, the acid derivatives were also less potent than their hydroxymethyl counterparts (YC-1, **1**). When the furan was converted into a benzene ring, the activity was significantly reduced.

However, introduction of an F atom at the R^3 position (**45f**) dramatically enhanced the inhibition of collagen-, AA- and PAF-induced aggregation but reduced the inhibitory effect on thrombin-induced aggregation. Methyl (**46e**) and methoxy (**45g**) substituted derivatives did not alter the platelet aggregation inhibition activity. The derivatives with bridging dioxomethylene groups significantly diminished the activity.

3.2. Hypoxia-inducible factor (HIF)

Hypoxia-inducible factor (HIF) is a transcription factor that induces the expression of various genes to resist tissue hypoxia.[4]

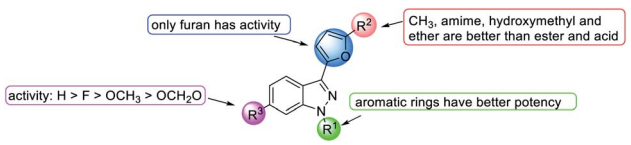

Fig. 13 Effects of the SAR of YC-1 analogs on antiplatelet activities.

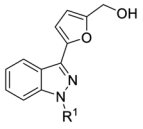

47

	HIF-1 transcriptional activity
YC-1 (**1**), R^1= benzyl	IC_{50}= 1.20 ± 0.50 μM
47a, R^1= Me	IC_{50}> 30.0 μM
47b, R^1= H	IC_{50}= 5.0 μM
47c, R^1= SO_2Ph	IC_{50}= 16.9 μM
47d, R^1= biphenly	IC_{50}= 3.3 μM
47e, R^1= 4-azidophenyl	IC_{50}= 1.24 ± 0.34 μM
47f, R^1= 2-(trifluoromethyl)benzyl	IC_{50}= 13.9 ± 0.39 μM
47g, R^1= 4-(trifluoromethyl)benzyl	IC_{50}= 9.40 ± 1.76 μM
47h, R^1= 4-cyanobenzyl	IC_{50}= 0.27 ± 0.01 μM
47i, R^1= 4-methoxybenzyl	IC_{50}= 0.97 ± 0.01 μM
26a, R^1= 2-fluorobenzyl	IC_{50}= 0.26 ± 0.01 μM
26b, R^1= 3-fluorobenzyl	IC_{50}= 0.48 ± 0.09 μM
26c, R^1= 4-fluorobenzyl	IC_{50}= 0.53 ± 0.09 μM
47j, R^1= 2,4-difluorobenzyl	IC_{50}= 0.31 ± 0.01 μM
47k, R^1= 2,6-difluorobenzyl	IC_{50}= 0.10 ± 0.01 μM
47l, R^1= 2,3,5,6-tetrafluorobenzyl	IC_{50}= 0.07 ± 0.01 μM
47m,R^1= 2,3,4,5,6-pentafluorobenzyl	IC_{50}= 0.18 ± 0.05 μM
47n, R^1= 2-chlorobenzyl	IC_{50}= 0.65 ± 0.06 μM
47o, R^1= 4-chlorobenzyl	IC_{50}= 2.80 ± 0.25 μM
26g, R^1= 2-pyridyl	IC_{50}= 0.30 ± 0.06 μM
26h, R^1= 3-pyridyl	IC_{50}= 0.46 ± 0.03 μM
47p, R^1= 4-pyridyl	IC_{50}= 0.83 ± 0.11 μM
47q, R^1= 4-azidomethylbenzyl	IC_{50}= 0.70 ± 0.08 μM
47r, R^1= 4-*N*-(prop-2-yn-1-yl)aminobenzyl	IC_{50}= 0.61 ± 0.09 μM

Fig. 14 The effect of YC-1 derivatives (**47**) on HIF-1 transcriptional activity.

Cellular adaptability to hypoxia is an important strategy for tumor survival.[44] In many studies, hypoxic conditions have been associated with malignancy in various cancers. Chemicals and drugs targeting HIF-1α have been discovered, and YC-1 is one of them. Moreover, under hypoxia conditions, YC-1 can inhibit HIF-1α activity and achieve anticancer effects.[3] As an inhibitor of HIF-1, YC-1 has manifested excellent effects in many different cancer cells,[45] including lung cancer,[4,5] bladder cancer,[46] breast cancer,[6] canine lymphoma,[47] chemoresistance,[8,9] colorectal cancer,[7] gastric carcinoma,[48,49] hepatocellular carcinoma cancer (HCC),[50–53] preeclampsia,[54] ovarian cancer,[55] and non-small cell lung cancer (NSCLC).[50,56–60]

In addition, HIF-1α is upregulated in lung parenchyma and alveolar macrophages in asthma and is also viewed as a major regulator of inflammation. YC-1 can inhibit the increase in HIF-1α expression controlling allergen-induced airway diseases in (AIAD) mice.[14] YC-1 can also decrease blood eosinophilia, the aryl hydrocarbon receptor (AHR), and allergic inflammatory gene expression: IL-13, IL-5, myeloperoxidase, and nitric oxide synthase (iNOS).[14]

However, YC-1 downregulated HIF-1α expression, a key component in osteogenesis, results in significant inhibition of regenerative bone formation.[61–63] In addition, YC-1 partially eliminates the protection ability of FG-4592, which stabilizes HIF-1α expression in spinal cord and PC-12 cells.[64]

Furthermore, under hypoxic/ischemic conditions in the brain, YC-1 can induce the regulatable subunit of HIF-1α, a potent therapeutic target in cerebral ischemia.[65] In 2011, Yan *et al.* found that inhibition of HIF-1 expression improves the ischemia-induced blood–brain barrier (BBB) disruption but does not influence brain edema.[66] Moreover, YC-1 suppressed the release of neutrophil, inflammatory factor and the activation of the HMGB1/TLR4/NF-NF-κB signaling pathway to protect BBB integrity.[67] Therefore, YC-1 has a protective effect on the cerebral vascular system.[66,67]

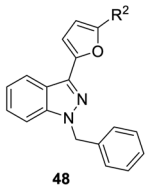

	HIF-1 transcriptional activity
YC-1 (**1**), R^2= CH_2OH	IC_{50}= 1.2 μM
48a, R^2= CH_2OAc	IC_{50}= 2.3 μM
48b, R^2= $CH_2OCOCH(CH_3)_2$	IC_{50}= 0.74 μM
48c, R^2= $CH_2OCOC(CH_3)_3$	IC_{50}= 0.89 μM
48d, R^2= CH_2N_3	IC_{50}> 30 μM
48e, R^2= CO_2Me	IC_{50}= 0.9 μM
48f, R^2= $CONH_2$	IC_{50}= 11.9 μM

Fig. 15 The effect of YC-1 derivatives (**48**) on HIF-1 transcriptional activity.

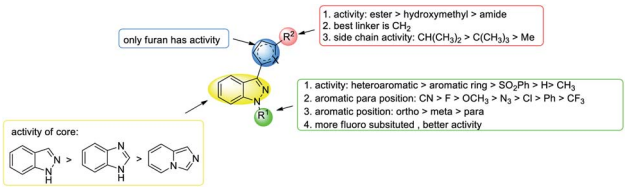

Fig. 16 SAR of YC-1 analogs for HIF-1 transcriptional activity.

HIF-1α also leads to an imbalance in the expression of the angiogenic protein that is considered to be the primary factor in hypoxic conditions prevalent in preeclampsia.[54,68] In 2015, Brownfoot *et al.* discovered that YC-1 significantly decreases soluble fms-like tyrosine kinase-1 (sFlt1), soluble endoglin (sENG) secretion and endothelial dysfunction in primary human tissues, which is a novel drug target for treating preeclampsia.[69]

The first structure–activity relationship study of YC-1 on HIF-1α inhibition in 2011 discussed the aromatic ring and the R^1 and R^2 functional groups of YC-1,[70] and in 2012, Takeuchi *et al.* further researched SAR studies of the N-terminal aromatic ring.[22]

In order to test the effects of YC-1 derivatives (**47–65**) on the inhibition of HIF-1 transcriptional activity, a cell-based HRE reporter gene assay was applied in HRE (X5)-Luc transfected HeLa cells. The main chemical modifications of the derivatives are located on the different substituents of heterocycles A, B, R^1, and R^2 (Fig. 2), including different heterocycles, electron donor or withdrawal groups, halide substitution, and other structures, which follow synthetic route a in Scheme 1 to give YC-1 derivatives (**47–48**). The SAR discussions are summarized in Fig. 14–16 and Schemes 5–8.

Firstly, the activity of pyridyl substitution was better than that of YC-1 (benzyl, **1**). Introduction of trifluoromethyl substitution (**47f–g**) at both the *para* and *ortho* positions resulted in reduced activity. In addition, fluorination was also an effective modification for inhibiting HIF-1 transcriptional activity. Among the monofluoro-substituted compounds (**26a–c**), *ortho* derivative **26a** showed better inhibitory activity than *meta* (**26b**) and *para* (**26c**) derivatives. In addition, *ortho*-difluoro-substituted derivative **47k** exhibited significant inhibition (IC_{50} = 0.10 μM) compared with *para*, *ortho*-difluoro-substituted derivative **47j** (IC_{50} = 0.31 μM). However, pentafluoro-substituted derivative **47m** also showed marked inhibition but was less potent than **47l**. These results indicated that fluoro substitution at the *ortho* position is crucial for inhibiting the transcriptional activity of HIF-1.

At the heterocycle B position, only furan substitution led to inhibitory activity. Other heterocycles, such as isoxazole, oxazole, thiazole, *etc.*, lost their inhibitory activity.

Almost all the R^2 altered substitutions displayed reduced activity, except for the esters. The ester derivatives (**48b**, **48c** and **48f**) had better inhibitory ability (IC_{50}: 0.74, 0.89 and 0.9 μM, respectively).

In addition, from 2014 to 2015, Chen *et al.*[71] and Masoud *et al.*[72] was based on YC-1 structure molecular modeling and synthesized two series of *N*-substituted indole derivatives **53** and **58** by using either a mixture of 1*H*-benzo[*d*]imidazol-2-amine (**49**) or 2-(azidomethyl)-1*H*-benzo[*d*]imidazole (**55**) and various benzyl bromide (**50**) in ethanol at room temperature to obtain intermediates **51** and **56**. Subsequently, the

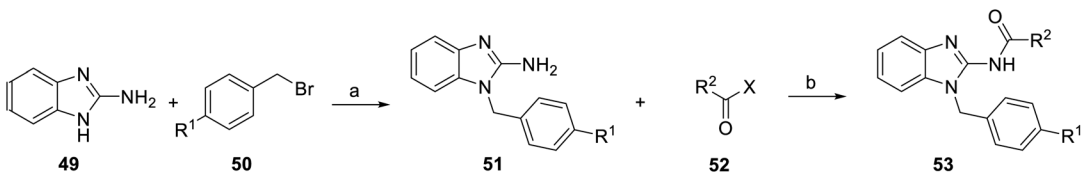

	HIF-1 transcriptional activity
YC-1 (**1**),	IC_{50}= 1.20 ± 0.50 μM
53a, R^1= Cl, R^2=4-fluorobenzyl	IC_{50}= 1.58 ± 0.75 μM
53b, R^1= Cl, R^2=4-chlorobenzyl	IC_{50}= 2.77 ± 1.39 μM
53c, R^1= Cl, R^2=4-bromobenzyl	IC_{50}= -
53d, R^1= Br, R^2=4-bromobenzyl	IC_{50}= 1.78 ± 0.75 μM
53e, R^1= Me, R^2=4-bromobenzyl	IC_{50}= -
53f, R^1= Me, R^2=4-(trifluoromethyl)benzyl	IC_{50}= -
53g, R^1= Me, R^2=4-methoxybenzyl	IC_{50}= -
53h, R^1= H, R^2=3-methylphenyl	IC_{50}= 0.60 ± 0.10 μM

Scheme 4 Synthesis and HIF-1 transcriptional activity effect of YC-1 analogs (**53**). Reagents and conditions: (a) KOH, EtOH, rt, 18 h; (b) EDCA, HOBt, DMF, rt, 24 h.

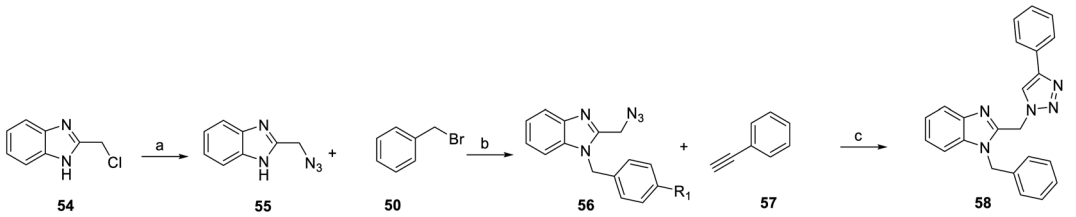

Scheme 5 Synthesis of YC-1 analogs (**58**). Reagents and conditions: (a) NaN_3, DMSO, rt, 5 h; (b) KOH, EtOH, rt, 18 h; (c) $CuSO_4 \cdot 5H_2O$, sodium ascorbate, DCM/water/*t*-BuOH, rt, 24 h.

intermediates were reacted with substituted acetyl halide (**52**) or substituted with ethynylbenzene (**57**) to produce **53** and **58** derivatives, respectively (Schemes 4 and 5).

Among the compounds (**53**) in this series, the most potent was **53h**, with an IC_{50} value of 0.6 μM (Scheme 4). For R^1 substituents, halogen substitution was more potent than alkyl substitution. For example, bromo substituted **53d** (IC_{50} = 1.78 μM) exhibited better inhibitory activity than methyl substituted derivatives (**53e–g**). In the R^2 position, fluoro-substituted **53a** exhibited better inhibitory activity (IC_{50} = 1.58 μM) than bromo- or chloro-substituted derivatives (**53b** and **53c**). Bioisosteric replacement of an amide linker to triazole ring (**58**) tended to extend conformational flexibility. However, none of the triazole series compounds (**58**) showed more than a 50% inhibition of HIF-1α expression.[72]

In 2016, Fuse *et al.* synthesized another series of imidazopyridine derivatives, **63** and **64**.[73] In this series, 1-iodoimidazo [1,5-*a*] pyridine (**59**) was used as the starting material, followed by Suzuki reaction to obtain compound **60**. Direct acylation catalyzed by $Pd(OAc)_2$ was applied for the formation of compounds **61** and **62**. Finally, sodium borohydride reduction was used to achieve final products **63** and **64** (Scheme 6).

In the SAR study (Scheme 6), derivatives **63b–63d** (IC_{50} = 39–75 μM) at the R^1 position containing electron-donating groups, such as methoxyphenyl and methylphenyl, had similar levels of inhibitory activity to **63a** (IC_{50} = 70 μM). Derivatives **63e–63g** containing electron-withdrawing compounds, such as (trifluoromethyl)phenyl and cyanophenyl, exerted higher levels of inhibitory activity. Despite the similar steric bulkiness of the substituents at the R^1 position, the inhibitory activity was **63d** (4-methoxyphenyl) < **63e** (4-(trifluoromethyl)phenyl) < **63g** (4-cyanophenyl) in increasing order. In the case of heterocycle X substitution, thiophene substituted **64** (IC_{50} = 3.7 μM) exerted a better effect than furan substituted **63a** (IC_{50} = 70 μM). However, these derivatives were all less potent than YC-1.

In conclusion, in terms of the core derivatives, indazole has better inhibitory activity than benzoimidazole and imidazopyridine. For heterocycle B substitution, only furan has HIF-1 inhibitory activity. Among the R^1 functional groups, the most effective is heterocyclic substitution. Furthermore, the best substitution position is the *ortho* position of the aromatic ring with fluoro substitution. Also, at the R^2 position, a hydroxymethyl group is a more effective substituent than the hydroxymethyl group. Finally, the most suitable side chain structure is isobutene (Fig. 16).

Recently, Fuse *et al.* synthesized indeno[2,1-*c*]pyrazolone compounds to test their HIF-1 transcriptional inhibitory activity *via* the use of a dual luciferase assay under hypoxic condition, as well as to test their antiproliferative activity using an MTT assay ((3-(4,5-dimethylthiazol-2-yl)-2,5-diphenyltetrazolium bromide)) in HeLa cells under normoxic conditions.[74]

Pyrazole (**65**) reacted with **66** to give 1-*N*-substituted pyrazole **67**. Compound **69** was obtained using nucleophilic addition from **67** and **68**, followed by cyclization to give compound **70** (Scheme 7).

Introduction of a nitrogen atom to the X position deteriorated HIF-1 inhibitory activity, for example, as in **70b**. In the R^1 position, the ring activating groups, such as methyl (**70c**), methoxy (**70d**) and hydroxy (**70e**), at the *para* position improved HIF-1 inhibition activity. These indeno[2,1-*c*]pyrazolones derivatives (**70**) didn't show strong toxicity, with the exception of compound **70e** (cytotoxicity IC_{50} = 2.2 μM). Compound **70e** showed impressive HIF-1 inhibitory activity and cytotoxicity under normoxic conditions, suggesting that other biological processes also contribute to antiproliferative effects.

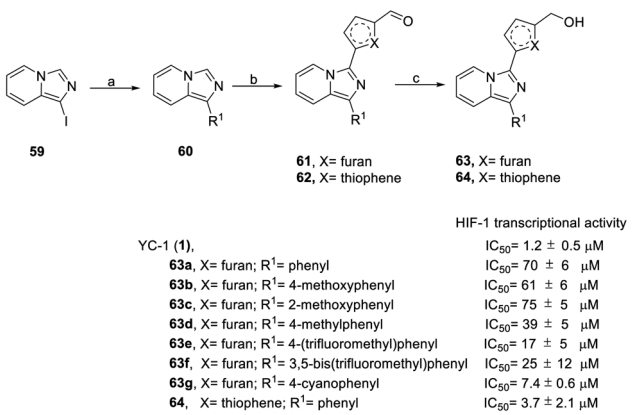

YC-1 (**1**),	HIF-1 transcriptional activity
63a, X= furan; R^1= phenyl	IC_{50}= 1.2 ± 0.5 μM
63b, X= furan; R^1= 4-methoxyphenyl	IC_{50}= 70 ± 6 μM
63c, X= furan; R^1= 2-methoxyphenyl	IC_{50}= 61 ± 6 μM
63d, X= furan; R^1= 4-methylphenyl	IC_{50}= 75 ± 5 μM
63e, X= furan; R^1= 4-(trifluoromethyl)phenyl	IC_{50}= 39 ± 5 μM
63f, X= furan; R^1= 3,5-bis(trifluoromethyl)phenyl	IC_{50}= 17 ± 5 μM
63g, X= furan; R^1= 4-cyanophenyl	IC_{50}= 25 ± 12 μM
64, X= thiophene; R^1= phenyl	IC_{50}= 7.4 ± 0.6 μM
	IC_{50}= 3.7 ± 2.1 μM

Scheme 6 Synthesis and HIF-1 transcriptional activity effect of YC-1 analogs (**63–64**). Reagents and conditions: (a) 5 mol% $Pd(PPh_3)_4$, arylboronic acids, K_2CO_3, 1,4-dioxane/H_2O, 110 °C, microwave, 1 h; (b) 5 mol% $Pd(OAc)_2$, 5-iodofuran-2-carbaldehyde (for **61**) or 5-bromothiophene-2-carbaldehyde (for **62**), CsOAc, 100 °C, microwave, 1.5 h; (c) $NaBH_4$, MeOH, rt, 5 min.

3.3. Vascular endothelial growth factor (VEGF)

Vascular endothelial growth factor (VEGF) is a signaling protein that stimulates blood vessel formation.[75] Without the nourishment of blood vessels, the size of a tumor mass cannot exceed 2

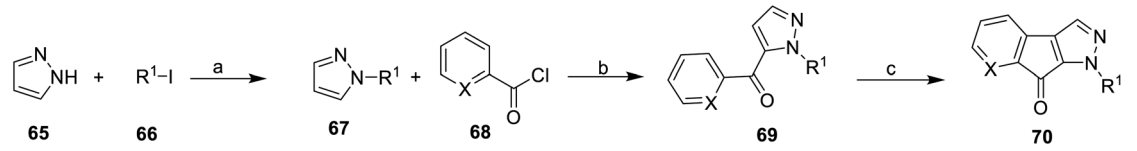

		Cytotoxicity	HIF-1	
YC-1 (**1**)	IC_{50}	56 ± 0.93	2.4 ± 0.51	μM
70a, X= C, R^1= Ph	IC_{50}	>10	1.4 ± 0.83	μM
70b, X= N, R^1= Ph	IC_{50}	52 ± 5.7	10 ± 0.46	μM
70c, X= C, R^1= 4-MePh	IC_{50}	>10	0.79 ± 0.16	μM
70d, X= C, R^1= 4-MeOPh	IC_{50}	>10	0.61 ± 0.10	μM
70e, X= C, R^1= 4-OHPh	IC_{50}	2.2 ± 0.067	0.39 ± 0.088	μM
70f, X= C, R^1= H	IC_{50}	>30	>30	μM

Scheme 7 Synthesis, cytotoxicity of HeLa cells and HIF-1 transcriptional activity of indeno[2,1-*c*]pyrazolones (**70**). Reagents and conditions: (a) Cu_2O, $CsCO_3$, DMF, 100 °C, 22 h; (b) *n*-BuLi, THF; (c) (i) K_2CO_3, ICl, $CHCl_3$, rt, 16 h; (ii) $Pd(PPh_3)_2Cl_2$, NaOAc, DMA, 130 °C, 20 h.

mm^3; therefore, angiogenesis is essential for tumor progression.[76,77] Additionally, the exudation process requires vascularization during metastasis.

Since VEGF is overexpressed in various human cancers and is released by a variety of tumor cells, it has been identified as the most important antiangiogenic factor contributing to tumor progression. When a drug can inhibit VEGF production or block its receptor signaling, it also leads to a significant inhibition of tumor growth, such as is the case with YC-1.

YC-1 blocks the induction of erythropoietin (EPO) and VEGF mRNA by inhibiting the hypoxia accumulation of HIF-1α under hypoxic conditions. According to studies by Yan *et al.*, in experimental central retinal venous occlusion (CRVO) in rhesus monkeys, the macular edema thickness was significantly decreased after YC-1 injection (90 μl, 200 μM) at 1 week. Meanwhile, the concentration of IL-6, IL-8, VEGF, the inflammation markers, were significantly decreased in YC-1 injection group. YC-1 showed anti-inflammatory and anti-angiogenesis-related expression and significantly alleviated macular edema.[16]

Temirak *et al.*, Abdullaziz *et al.* synthesized a series of YC-1 analogs **73–78** (Scheme 8) and discussed the SAR with cytotoxicity and VEGF levels.[78–80]

1,2-Phenylenediamine (**71**) was condensed with furfural compound **72** in *p*-toluenesulfonic acid and DMF to obtain 5-methyl derivatives **73**. Then, compound **73** was reacted with various chloro compounds with K_2CO_3 in acetone at room temperature to give *N*-substituted product **74**. Under the same reaction conditions, treatment of 1*H*-benzimidazoles **73** with ethyl bromoacetate can provide *N*-alkylated products **75**. Next, compound **76** was obtained from compound **75** with hydrazine hydrate in ethanol. Compound **76** was reacted with potassium hydroxide (KOH) and ethanol to obtain compound **77**. Hydrazide compound **76** was cyclized with carbon disulfide in potassium hydroxide and ethanol to obtain oxadiazole ring compound **78** (Scheme 8).

Benzimidazole derivatives (**73–78**) were tested for cytotoxicity in MCF-7 human breast cancer cells. An ELISA kit was used to measure the level of human VEGF in MCF-7 cells, and the inhibition percentage was calculated based on the level of untreated cells.[81,82] The SAR was discussed based on the R^1, R^2, R^3 positions and aromatic substituents, as shown in Fig. 17–19.[78–80]

The results showed that steric effect has an extreme impact on the R^1 position. Conversion to methyl at the R^1 position significantly enhanced VEGF inhibition activity. For example, R^1 methyl compounds **74c** significantly enhanced VEGF inhibition (VEGF inhibition was 97%), and VEGF inhibition of hydrogen compounds **74b** and **76b** ranged from 14–23%.

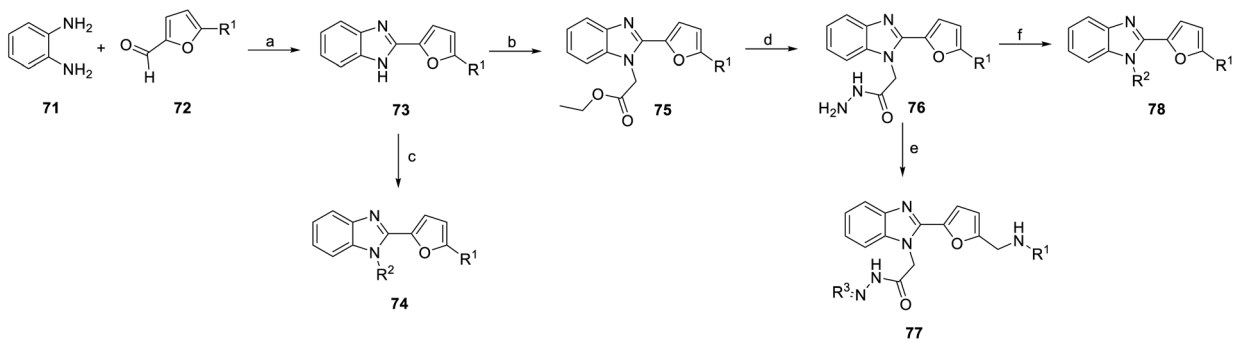

Scheme 8 Synthesis of benzimidazole derivatives (**73–78**). Reagents and conditions: (a) *p*-TsOH, DMF, 100 °C; (b) ethyl bromoacetate, K_2CO_3, acetone, rt; (c) chloro compounds, K_2CO_3, acetone, rt; (d) NH_2NH_2, ethanol, 90 °C; (e) EtOAc, KOH, ethanol, reflux; (f) CS_2, KOH, ice followed by reflux.

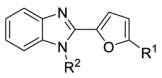

74-75

		MCF-7 IC_{50} (μg/ml)	VEGF level (Pg/ml)	Inhibition (%)
74a, R^1= H;	R^2= benzyl	6.98	90.70	(98%)
74b, R^1= H;	R^2= phenylsulfonyl	21.20	4514.23	(14%)
74c, R^1= CH_3;	R^2= phenylsulfonyl	8.63	125.18	(97%)
74d, R^1= H;	R^2= CH_2CN	19.52	2987.11	(39%)
74e, R^1= H;	R^2= CH_3	21.50	280.24	(95%)
74f, R^1=morpholinomethyl;	R^2=H	15.43	1329.61	(58%)
75a, R^1= H;	R^2= $CH_2COOCH_2CH_3$	15.20	2000.82	(62%)
75b, R^1= CH_3;	R^2= $CH_2COOCH_2CH_3$	17.80	3760.70	(28%)
DMSO			5250.00	(-)

Fig. 17 Effects of the compounds **74–75** on the MCF-7 breast cancer cell line and the VEGF level (pg mL^{-1}) in the MCF-7 breast cancer cell line.

Morpholinomethyl substitution **74f** led to a moderate inhibition effect. At the R^2 position, the conversion of hydrogen to benzyl significantly increased the activity (**74a**, VEGF inhibition = 98%). The cyanomethyl compound (**74d**) slightly decreased VEGF inhibition activity. Conversion into ethoxy methanoneyl (**75**) diminished the activity, where VEGF inhibition ranged from 28–62% (Fig. 17).

When the N-terminal functional group was converted to hydrazineyl, benzoylhydrazineyl, benzylhydrazineyl and methylcarbamothioylhydrazineyl substitutions, the derivatives had weak anticancer activity, such as compounds **76a–d**. On the other hand, phenyl at the R^3 position (**77a**, VEGF inhibition = 5%) had no VEGF inhibition activity, but phenyls with substitutes were potent functional groups for VEGF inhibition (**77b–d**, VEGF inhibition was above 96%). Conversion to a heterocycle at the R^3 position decreased activity, including pyridine (**77e**, VEGF inhibition 58%) and furan (**77f**, VEGF inhibition 30%). Side chains at the R^3 position played important roles in inhibitory activity. For instance, methyl side chains of compounds **77g** and **77h** led to worse VEGF inhibition (VEGF inhibition = 31% and 19%, respectively) (Fig. 18).

Finally, replacement of the R^2 position with a heterocycle dramatically reduced the inhibitory potency of VEGF, where VEGF inhibition was less than 41%, including oxadiazole (**78b**, **78c**, **78d**), thiadiazole (**78e**) and imidazole (**78f**). However, some

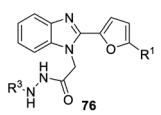

76

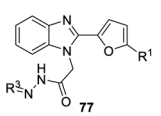

77

		MCF-7 IC_{50}(μg/ml)	VEGF level (Pg/ml)	Inhibition (%)
76a, R^1= H;	R^3= H	20.20	4010.45	(23%)
76b, R^1= CH_3;	R^3=H	22.40	760.40	(85%)
76c, R^1=H;	R^3= CONHPh	16.00	2300.14	(56%)
76d, R^1=H;	R^3= COPh	22.10	4800.00	(9%)
76e, R^1=H;	R^3= CH_2Ph	21.80	4670.23	(11%)
76f, R^1=H;	R^3= $COCH_3$	18.70	4050.45	(23%)
76g, R^1=H;	R^3= $CSNHCH_3$	17.50	2600.40	(51%)
77a, R^1=H;	R^3= CH(Ph)	37.90	5000.40	(5%)
77b, R^1=H;	R^3= CH(4-CH_3Ph)	11.80	196.80	(96%)
77c, R^1=H;	R^3= CH(4-OCH_3Ph)	8.63	196.76	(96%)
77d, R^1=H;	R^3= CH(4-ClPh)	11.20	184.30	(97%)
77e, R^1=H;	R^3= CH(3-pyridine)	15.40	2190.66	(58%)
77f, R^1=H;	R^3= CH(2-furan)	16.60	3700.00	(30%)
77g, R^1=H;	R^3= CCH_3(Ph)	16.00	3600.90	(31%)
77h, R^1=H;	R^3= CCH_3(4-OHPh)	21.80	4230.50	(19%)
77i, R^1=H;	R^3= CCH_3(4-CH_3Ph)	7.80	104.30	(98%)
DMSO			5250.00	(-)

Fig. 18 Effect of the compounds **76–77** on the breast cancer cell line MCF-7 and the VEGF level (pg mL^{-1}) in the breast cancer cell line MCF-7.

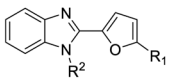

78

	MCF-7 IC_{50}(μg/ml)	VEGF level (Pg/ml)	Inhibition (%)
78a, R^1= H; R^2=	20.50	480.45	(91%)
78b, R^1= H; R^2=	16.90	3112.78	(41%)
78c, R^1= CH_3; R^2=	16.60	3200.80	(39%)
78d, R^1= H; R^2=	19.30	4420.70	(16%)
78e, R^1= H; R^2=	21.30	4195.46	(14%)
78f, R^1= H; R^2=	24.52	3790.38	(22%)
78g, R^1= H; R^2=	9.39	535.90	(86%)
78h, R^1= H; R^2=	11.41	362.80	(92%)
78i, R^1= H; R^2=	8.29	210.60	(96%)
DMSO		5250.00	(-)

Fig. 19 Effects of the compounds **78** on the MCF-7 breast cancer cell line and the VEGF level (pg mL^{-1}) in the breast cancer MCF-7 cell line.

of heterocycles in the R^2 position retained inhibitory effects, such as a 91% and 86% inhibition on triazole (**78a**) and thiazolidine (**78g**), respectively. In addition, heterocycles with a side chain can improve activity. For example, 2-ethoxy-2-oxoethyl (**78h**) and 2-hydrazineyl-2-oxoethyl (**78i**) displayed excellent inhibitory activity on VEGF levels (92% and 96%, respectively).

The SAR of benzimidazole derivatives on VEGF inhibition is summarized in Fig. 20. At the R^1 position, methyl was best for VEGF inhibitory activity. However, the R^2 position needs to maintain an aromatic ring or heterocycle with a side chain to have good activity.

3.4. Nuclear factor kappa light chain enhancer of activated B cells (NF-κB)

In 2014, Kuo *et al.* synthesized a series of YC-1 analogs **79** and discussed the SAR with osteoclast inhibition.[83] To examine the

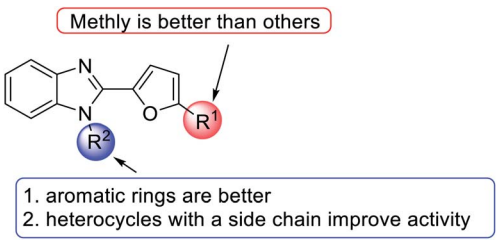

Fig. 20 Effects of the SAR of benzimidazole derivatives on VEGF inhibition.

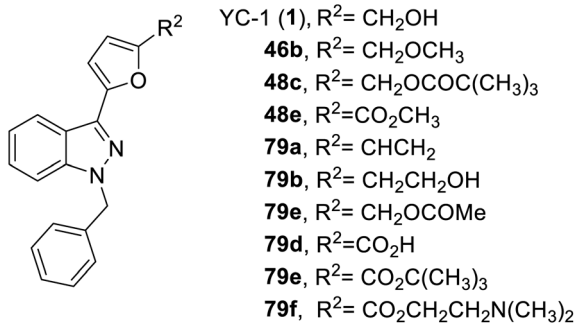

Fig. 21 Structure of YC-1 analogs (**48**, and **79**).

effects of the inhibitory activity of each derivative on osteoclast formation, each derivative was added to bone marrow-derived osteoclasts (from male rats) for testing. In the presence of RANKL (50 ng mL^{-1}) and M-CSF (20 ng mL^{-1}), 10 μM of different test compounds were added for 5 days. After 5 days, the formation of osteoclasts was confirmed using tartrate-resistant acid phosphatase staining (TRAP staining). Among these derivatives, only **79f**, with a furan ring and 2-(dimethylamino)ethyl, inhibited osteoclastogenesis by over 90% (Fig. 21).

4. Conclusions

Since YC-1 was discovered in 1994, there have been discussions on many related physiological activities as well as SAR. Riociguat was even developed based on YC-1 activity. The 83 articles, including 4 patent literatures, selected and discussed in this article confirm its wide use.

In this review, we summarized the synthetic strategies of YC-1 derivatives based on various substituents of YC-1, systematically reviewed their biological activities, including sGC, HIF-1, VEGF, and NF-κB, and described the SAR in detail. Many chemists have modified the compound structures associated with these pharmacological activities to obtain more derivatives with greater biological activity in areas including anticancer, reverse chemoresistance, neovascularization, neural protection, asthma, learning and memory, and bone formation. However, most of the studies were on HIF-1 and sGC. The latest research indicated that YC-1 and NF-κB inhibition are significantly related, but there are few relevant studies. We believe that the inhibition of NF-κB by YC-1 derivatives is worth focusing on.

From a future perspective, to promote the innovation of YC-1 analog drugs, green, combinatorial, and diversity-oriented synthetic methods are essential for developing large-scale analog libraries for high-throughput drug screening and SAR research. In addition, although YC-1 has a wide range of applications, no studies have focused on molecular docking methods. Relevant studies in the future will help to explain the related multipharmacology and will also lead to the discovery of relevant multitarget drugs for clinical use.

Author contributions

Data curation, K.-H. Y., investigation, K.-H. Y., H.-Y. H. Project administration, H.-Y. H.; resources, H.-Y. H.; supervision, H.-Y. H.; writing – original draft, K.-H. Y.; writing – review and editing, H.-Y. H. All authors have read and agreed to the published version of the manuscript.

Conflicts of interest

There are no conflicts to declare.

Notes and references

1 C. C. Wu, F. N. Ko, S. C. Kuo, F. U. Lee and C. M. Teng, *Blood*, 1994, **84**, 4226–4233.
2 J. C. Lien, F. Y. Lee, L. J. Huang, T. M. Huang, S. C. Tsai, C. M. Teng, C. C. Wu, F. C. Cheng and S. C. Kuo, *J. Med. Chem.*, 2001, **44**, 3746–3749.
3 E. J. Yeo, Y. S. Chun, Y. S. Cho, J. Kim, J. C. Lee, M. S. Kim and J. W. Park, *J. Natl. Cancer Inst.*, 2003, **95**, 516–525.
4 T. Bollinger, S. Gies, J. Naujoks, L. Feldhoff, A. Bollinger, W. Solbach and J. Rupp, *J. Leukocyte Biol.*, 2014, **96**, 305–312.
5 T. C. Hsia, W. H. Liu, W. W. Qiu, J. Luo and M. C. Yin, *Molecules*, 2014, **19**, 19892–19906.
6 L. Bergandi, S. Canosa, G. Pittatore, F. Silvagno, S. Doublier, G. Gennarelli and C. Benedetto, *Biol. Reprod.*, 2019, **100**, 1521–1535.
7 X. Li, J. Xing, H. Wang and E. Yu, *Biosci. Rep.*, 2019, **39**(5), BSR20180268.
8 W. L. Chen, C. C. Wang, Y. J. Lin, C. P. Wu and C. H. Hsieh, *J. Transl. Med.*, 2015, **13**, 389–402.
9 S. Kaowinn, I. R. Cho, J. Moon, J. Soh, H. Y. Kang, C. R. Jung, S. Oh, H. Song, S. S. Koh and Y. H. Chung, *Int. J. Oncol.*, 2015, **46**, 2076–2082.
10 J. Wu, X. Ke, N. Ma, W. Wang, W. Fu, H. Zhang, M. Zhao, X. Gao, X. Hao and Z. Zhang, *Drug Des., Dev. Ther.*, 2016, **10**, 3071–3081.
11 X. Ke, J. Wu, W. Wang, H. Zhang, N. Ma, W. Fu, M. Zhao, X. Gao, X. Hao and Z. Zhang, *Int. J. Biol. Sci.*, 2016, **12**, 1363–1371.
12 X. Li, N. Lu, R. Tan, J. An, Z. Cai, X. Hu, F. Wang, H. Wang, C. Lu and H. Lu, *J. Mol. Neurosci.*, 2018, **66**, 238–250.
13 W. T. Lee, S. H. Tai, A. C. Lee, Y. W. Lin, H. Y. Hung, S. Y. Huang, Y. S. Wu and E. J. Lee, *Mol. Med. Rep.*, 2018, **17**, 6490–6496.
14 E. McEachern, C. Dewitz, S. Shin, K. Akong, D. G. Nagle, D. H. Broide, P. Akuthota and L. E. Crotty Alexander, *J. Clin. Immunol.*, 2017, **176**, 94–99.
15 Y. Liang, C. E. Carroll, I. Benakanakere, C. Besch-Williford and S. M. Hyder, *Int. J. Oncol.*, 2013, **4**, 179–187.
16 J. An, Z. Yan, Q. Shang, N. Zhou and J. Ma, *Curr. Eye Res.*, 2018, **43**, 526–533.
17 W. S. Lee, M. S. Chang, B. C. Chen, J. R. Sheu and C. H. Lin, *Mol. Pharmacol.*, 2004, **66**, 561–571.
18 K. C. Liang, W. L. Chien, C. M. Teng, S. C. Kuo, F. Y. Lee and W. M. Fu, *Mol. Pharmacol.*, 2003, **63**, 1322–1328.
19 C. B. Yeh, J. W. Wang, S. J. Chou, K. C. Lu, T. H. Chu, W. Y. Chen, J. L. Chien, M. H. Yen, T. H. Chen and J. F. Shyu, *J. Bone Miner. Metab.*, 2018, **36**, 508–518.

20 Y. S. Chun, E. J. Yeo and J. W. Park, *Cancer Lett.*, 2004, **207**, 1–7.
21 C. H. Wu, C. H. Pan and M. J. Sheu, *Vasc. Biol.*, 2019, **5**, DOI: 10.5772/intechopen.84572.
22 M. Hori, A. Takeuchi, S. Sato, H. S. Ban, T. Kuchimaru, S. Kizaka-Kondoh, T. Yamori and H. Nakamura, *Med. Chem. Commun.*, 2012, **3**, 1455–1461.
23 T. Meng, K. Yuanfang and C. Bingje, *China Patent*, 106316958A, 2015.
24 C. M. Counceller, C. C. Eichman, B. C. Wray, C. Brenda and J. P. Stambuli, *Org. Lett.*, 2008, **10**, 1021–1023.
25 J. C. Lien, F. Y. Lee, L. J. Huang, T. M. Huang, S. C. Tsai, C. M. Teng, C. C. Wu, F. C. Cheng and S. C. Kuo, *J. Med. Chem.*, 2001, **44**, 3746–3749.
26 A. Straub, C. Furstner, U. Niewohner, T. Jaetsch, A. Feurer, R. Kast, J. P. Stasch, E. Perzborn, J. Hutter and K. Dembowsky, *European Patent*, EP0932403A1, 1996.
27 V. Collot, P. Dallemagne, B. Patrick, R. Philippe and S. Rault, *Tetrahedron*, 1999, **55**, 6917–6922.
28 K. W. Hering, J. D. Artz, W. H. Pearson and M. A. Marletta, *Bioorg. Med. Chem. Lett.*, 2006, **16**, 618–621.
29 X. Yang, J. Yu, C. Wu and W. Su, *J. Org. Chem.*, 2020, **85**, 1009–1021.
30 C. M. Teng, F. Y. Lee and S. C. Kuo, *US Pat.*, US 7345079B2, 2002.
31 M. Katsuno, K. Inamoto, T. Yoshino, L. Suzuki, K. Hiroya and T. Sakamoto, *Chem. Lett.*, 2004, **33**(8), 1026–1027.
32 K. Inamoto, M. Katsuno, T. Yoshino, Y. Arai, K. Hiroya and T. Sakamoto, *Tetrahedron*, 2007, **63**, 2695–2711.
33 O. V. Evgenov and J. P. Stasch, *Handb. Exp. Pharmacol.*, 2013, **218**, 279–313.
34 S. C. Kuo, F. Y. Lee and C. M. Teng, *US Pat*, US5574168A, 1996.
35 T. Utkan, I. Komsuoglu Celikyurt, C. Ozer, N. Gacar and F. Aricioglu, *Med. Sci. Monit. Basic Res.*, 2014, **20**, 130–137.
36 K. C. Liang, W. L. Chien, C. M. Teng, S. C. Kuo, F. Y. Lee and W. M. Fu, *Eur. J. Neurosci.*, 2005, **21**, 1679–1688.
37 K. C. Liang, W. L. Chien and W. M. Fu, *Eur. J. Pharmacol.*, 2008, **590**, 233–240.
38 D. A. Tulis, *Curr. Med. Chem.*, 2004, **2**, 343–359.
39 K. J. Peyton, X. M. Liu, N. N. Mendelev, H. Wang, D. A. Tulis and W. Durante, *Mol. Pharmacol.*, 2009, **75**, 208–217.
40 W. C. Chang, C. H. Wu, G. Y. Chang, S. C. Kuo and C. M. Teng, *J. Pharmacol. Sci.*, 2004, **94**, 252–260.
41 A. Straub, J. P. Stasch, A. A. Cristina, B. B. Jordi, B. Ducke, A. Feurer and C. Fürstner, *Bioorg. Med. Chem. Lett.*, 2001, **11**, 781–784.
42 F. Y. Lee, J. C. Lien, L. J. Huang, S. L. Pan, J. H. Guh, C. M. Teng and C. C. Kuo, *J. Med. Chem.*, 2002, **45**, 4947–4949.
43 S. Weigand, J. Mittendorf, C. Alonso-Alija, E. Bischoff, A. Feurer, M. Gerisch, A. Kern, D. Knorr, D. Lang, K. Muenter, M. Radtke, H. Schirok, K. H. Schlemmer, E. Stahl, A. Straub, F. Wunder and J. P. Stasch, *ChemMedChem*, 2009, **4**, 853–865.
44 P. Vaupel and M. Höckel, *J. Natl. Cancer Inst.*, 2001, **93**, 266–276.
45 T. Harada, K. Hirose, Y. Wada, M. Sato, K. Ichise, M. Aoki, T. Kato, K. Takeda and Y. Takai, *J. Radiat. Res.*, 2020, **61**, 524–534.
46 C. L. Shui, C. Liu, Q. Wang, H. Luo and C. G. Gu, *Braz. J. Med. Biol. Res.*, 2017, **51**, e6768–e6775.
47 M. Igase, S. Kambayashi, K. Kobayashi, A. Kimura, T. Shimokawa Miyama, K. Baba, S. Noguchi, T. Mizuno and M. Okuda, *J. Vet. Med. Sci.*, 2015, **77**, 1405–1412.
48 R. X. Wang, X. W. Ou, M. E. Kang and J. Q. Shi, *Eur. Rev. Med. Pharmacol. Sci.*, 2018, **22**, 8237–8247.
49 Y. Kitajima, K. Wakiyama, T. Tanaka, M. Kaneki, K. Yanagihara, S. Aishima, J. Nakamura and H. Noshiro, *Sci. Rep.*, 2017, **7**, 12653–12665.
50 J. Wu, P. Li, L. Zhao and X. W. Feng, *Sleep Breath.*, 2016, **20**, 167–173.
51 J. Kong, X. Ding, W. Xu, S. Dong, Y. Du, C. Yao, J. Gao, S. Ke, S. Wang and W. Sun, *Oncol. Lett.*, 2018, **16**, 5230–5236.
52 Y. Liu, X. Wan, Y. Zhao, X. Sun, D. Fan and L. Guo, *PLoS One*, 2017, **12**, e0184213.
53 X. Li, W. Zhao and Z. Li, *Pharmazie*, 2017, **71**, 524–529.
54 Y. Zhang, H. J. Zhao, X. R. Xia, F. Y. Diao, X. Ma, J. Wang, L. Gao, J. Liu, C. Gao, Y. G. Cui and J. Y. Liu, *Clin. Chim. Acta*, 2019, **489**, 203–211.
55 P. Lin, L. Sun, Z. Qin, Y. Liu, L. L. Deng and C. Lu, *Exp. Biol. Med.*, 2015, **240**, 1434–1445.
56 H. Hu, X. K. Miao, J. Y. Li, X. W. Zhang, J. J. Xu, J. Y. Zhang, T. X. Zhou, M. N. Hu, W. L. Yang and L. Y. Mou, *Eur. J. Pharmacol.*, 2020, **874**, 172961–172977.
57 J. Sakakibara-Konishi, Y. Ikezawa, H. Mizugaki, S. Oizumi and M. Nishimura, *Int. J. Clin. Oncol.*, 2017, **22**, 59–69.
58 F. Takahashi, F. Nurwidya, I. Kobayashi, A. Murakami, M. Kato, K. Minakata, T. Nara, M. Hashimoto, S. Yagishita, H. Baskoro, M. Hidayat, N. Shimada and K. Takahashi, *Biochem. Biophys. Res. Commun.*, 2014, **455**, 332–338.
59 J. Zhou, Q. Jin, X. Xu, F. Huang and W. Xu, *Oncol. Lett.*, 2019, **1**, 4034–4043.
60 W. Wu, J. Wan, Y. Huang, W. Ge and S. Liu, *Oncol. Rep.*, 2016, **36**, 659–668.
61 L. Ye, C. Zhou, C. Jiang, J. Bai, Y. Chi and H. Zhang, *Tumor Biol.*, 2015, **36**, 9179–9188.
62 H. Furusho, H. Sasaki, D. B. Rider, J. M. Dobeck, W. P. Kuo, A. Fujimura, S. Yoganathan, K. Hirai, S. Xu, K. Sasaki and P. Stashenko, *J. Endod.*, 2019, **45**, 181–188.
63 J. Shao, C. Wan, S. R. Gilbert, R. C. Riddle, F. Long, R. S. Johnson, E. Schipani and T. L. Clemens, *Ann. N. Y. Acad. Sci.*, 2010, **1192**, 322–326.
64 K. Zhou, K. Wu, Y. Wang, Y. Zhou, N. Tian, Y. Wu, D. Chen, D. Zhang, X. Wang, H. Xu and X. Zhang, *Brain Res.*, 2016, **163**, 19–26.
65 Y. Tang, M. Bernaudin, M. Reilly, E. Petit and F. R. Sharp, *J. Biol. Chem.*, 2002, **277**, 39728–39738.
66 J. Yan, B. Zhou, S. Taheri and H. Shi, *PLoS One*, 2011, **6**, e27798–e27808.
67 L. Kong, Y. Ma, Z. Wang, N. Liu, G. Ma, C. Liu, R. Shi and G. Du, *Int. Immunopharmacol.*, 2021, **94**, 107507–107519.
68 H. M. Brandon, A. Rajakumar, A. Daftary, R. Ness and K. P. Conrad, *Placenta*, 2004, **25**, 763–769.

69 S. Tong, F. C. Brownfoot, N. J. Hannan, R. Hastie, P. Cannon, L. Tuohey and T. J. Kaitu'u-Lino, *Mol. Cell. Endocrinol.*, 2015, **41**, 202–208.
70 N. J. Kim, H. An, J. W. Jung, H. Jang, J. W. Park and Y. G. Suh, *Bioorg. Med. Chem. Lett.*, 2011, **21**, 6297–6300.
71 J. Wang, J. Chen, P. Schwab, K. T. Park, T. N. Seagroves, L. K. Jennings, D. D. Miller and W. Li, *Anticancer Res.*, 2014, **34**, 3891–3904.
72 J. Wang, G. N. Masoud, J. Chen, D. Miller and W. Li, *Anticancer Res.*, 2015, **35**, 3849–3859.
73 S. Fuse, T. Ohuchi, Y. Asawa, S. Sato and H. Nakamura, *Bioorg. Med. Chem. Lett.*, 2016, **26**, 5887–5890.
74 S. Fuse, K. Suzuki, T. Kuchimaru, T. Kadonosono, H. Ueda, S. Sato, S. Kizaka-Kondoh and H. Nakamura, *Bioorg. Med. Chem.*, 2020, **28**, 115207–115213.
75 S. J. Galli, D. R. Senger, A. M. Dvorak, C. A. Perruzzi, V. S. Harvey and H. F. Dvorak, *Science*, 1983, **219**, 983–985.
76 M. O'Reilly, S. Parangi, G. Christofori, L. Holmgren, J. Grosfeld, J. Folkman and D. Hanahan, *Proc. Natl. Acad. Sci. U.S.A.*, 1996, **93**, 2002–2007.
77 L. Holmgren, M. S. O'Reilly and J. Folkman, *Nat. Med.*, 1995, **1**, 149–153.
78 A. Temirak, Y. M. Shaker, F. A. F. Ragab, M. M. Ali, S. M. Soliman, J. Mortier, G. Wolber, H. I. Ali and H. I. El Diwani, *Arch. Pharm.*, 2014, **347**, 291–304.
79 Y. M. Shaker, A. Temirak, F. A. Ragab, M. M. Ali, H. I. Ali and H. I. El Diwani, *Eur. J. Med. Chem.*, 2014, **87**, 868–880.
80 M. A. Abdullaziz, H. T. Abdel-Mohsen, A. M. El Kerdawy, F. A. F. Ragab, M. M. Ali, S. M. Abu-bakr, A. S. Girgis and H. I. El Diwani, *Eur. J. Med. Chem.*, 2017, **136**, 315–329.
81 P. Skehan, R. Storeng, D. Scudiero, A. Monks, J. McMahon, D. Vistica, J. T. Warren, H. Bokesch, S. Kenney and M. R. Boyd, *J. Natl. Cancer Inst.*, 1990, **82**, 1107–1112.
82 A. Monks, D. Scudiero, P. Skehan, R. Shoemaker, K. Paull, D. Vistica, C. Hose, J. Langley, P. Cronise, A. Vaigro-Wolff, M. Gray-Goodrich, H. Campbell, J. Mayo and M. Boyd, *J. Natl. Cancer Inst.*, 1991, **83**, 757–766.
83 T. H. Lin, T. H. Kuo, R. S. Yang, S. C. Kuo, W. M. Fu and H. Y. Hung, *J. Med. Chem.*, 2015, **58**, 4954–4963.